A simple model of the effects of the mid-latitude total ion trough in the bottomsideFlayer on HF radiowave propagation

Article

Published Version

It is advisable to refer to the publisher's version if you intend to cite from the work. See Guidance on citing.

A simple model of the effects of the mid-latitude total ion trough in the bottomside *F* layer on HF radiowave propagation

Michael Lockwood[1]

Radio Research Centre, Auckland University, New Zealand

Observations of the amplitudes and Doppler shifts of received HF radio waves are compared with model predictions made using a two-dimensional ray-tracing program. The signals are propagated over a sub-auroral path, which is shown to lie along the latitudes of the mid-latitude trough at times of low geomagnetic activity. Generalizing the predictions to include a simple model of the trough in the density and height of the *F*2 peak enables the explanation of the anomalous observed diurnal variations. The behavior of received amplitude, Doppler shift, and signal-to-noise ratio as a function of the K_p index value, the time of day, and the season (in 17 months of continuous recording) is found to agree closely with that predicted using the statistical position of the trough as deduced from 8 years of Alouette satellite soundings. The variation in the times of the observation of large signal amplitudes with the K_p value and the complete absence of such amplitudes when it exceeds 2.75 are two features that implicate the trough in these effects.

1. INTRODUCTION

The 'main,' or 'mid-latitude,' trough is known to be a regular feature of the topside ionosphere [e.g., *Ahmed et al.,* 1979]. The morphology of this region of depleted ionospheric plasma during geomagnetically quiet periods has been reviewed by *Mendillo and Chacko* [1977]. It is not only observed in the plasma density at any one altitude but also in the total content [*Buonsanto et al.,* 1979]. The depth of the trough is height dependent, the poleward wall being a more prominent feature at lower altitudes [*Ahmed et al.,* 1979]. Although the depletion is known to persist to altitudes below the *F*2 peak, observations of a bottomside trough remain comparatively rare. This is mainly due to the effects of 'off-vertical' reflections on conventional ground-based ionosondes [*Nygrén,* 1977]. As a result of such effects the trough can only be resolved if it is exceptionally wide (under very quiet geomagnetic conditions) or if the ionosonde has a direction-finding capability. The ground-based, airborne, and satellite observations of the trough below the *F*2 peak that have been made, have been

reviewed by *Hartmann* [1975] and *Lockwood* [1980].

Statistically, the center of the trough lies near the ionospheric projection of the equatorial magnetospheric plasmapause, and the two move equatorward at times of increasing magnetic activity in a similar manner [*Köhnlein and Raitt,* 1977]. At any one instant, however, the plasmapause, the light ion trough, and the total ion trough do not always coincide [*Grebowsky et al.,* 1978]. Various mechanisms producing the depletion have been theorized. *Schunk et al.* [1976] invoked enhanced loss rates due to high-latitude convective motions. The trough at an altitude of 300 km was observed to be deepest in the dusk sector on quiet winter nights by *Brinton et al.* [1978]. This implies that normal loss processes may be occurring at times, exceptionally low concentrations arising where the corotation and convective electric fields oppose each other, giving long periods of time in which the plasma decays [*Spiro et al.,* 1978]. These and other theories all indicate that the trough should also be present in the bottomside *F* layer [*Lockwood,* 1980].

The morphology of the northern hemisphere trough in the *F*2 peak density has been studied and several numerical models developed [e.g., *Feinblum,* 1973]. *Halcrow and Nisbet* [1977] used a data set of 29,770 soundings taken by the Alouette I and II topside sounders between 1962 and 1970.

[1]Present address: Rutherford and Appleton Laboratories, Ditton Park, Slough SL3 9JX, Berks, England.

2. DATA AND ANALYSIS

The data used in this study are observations of the Doppler shifts and power losses of HF radio waves received after propagating over a mid-latitude path. The path lies approximately west to east geomagnetically and has a great circle length of 5.212 km. The signals are transmitted from Ottawa, Canada (geographic coordinates 45°18'N, 75°45'W), at a power of 10 kW and received at the Sir Norman Lockyer Observatory, Sidmouth, England (50°41'N, 3°13'W). They are 7.335-MHz CW signals transmitted by a vertical monopole antenna and are received on parallel Beverage antennae, using a 1-kHz receiver bandwidth.

The predicted invariant latitudes Λ of the tops and bases of the trough walls are shown in Figure 1 as a function of local time (LT) for the night of May 18–19, 1976 (mean K_p value $\bar{K}_p = 1.1$). These predictions are made using the regression equations derived by *Halcrow and Nisbet* [1977] (hereinafter referred to as 'H and N'). The positions of the sunrise and sunset ends of the trough are predicted using the mean solar zenith angle expressions deduced by *Feinblum* [1973]. These regression equations cannot be used as accurate indicators of the trough's position at any one instant [*Mendillo et al.*, 1978], and their use here is, therefore, merely to show that observed features are consistent with the mean statistical morphology of the trough in the $F2$ peak. In Figure 1 the orientations of the propagation path at various universal times (UT) are also shown. The points A and B are 0.25 and 0.75 of the path length from Ottawa (O), respectively, and at an altitude of 200 km. It can be seen
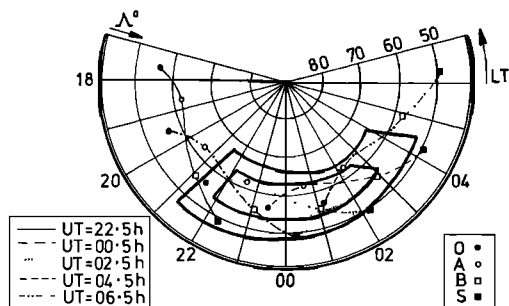
that at this low K_p value the mean trough passes over the entire length of this path.

In order to predict the effects of a trough on the Doppler shift and amplitude at Sidmouth (S), use was made of a two-dimensional, Snell's law-based, ray-tracing program. The ionization profile adopted was a two-parabola model, with a linear concentration increase between the peak of the E layer and the bottomside F layer [*Bradley and Dudeney*, 1973]. The peak heights and densities used were taken from the CCIR [1966] model. The trough was included by using a correction factor Φ defined by

$$\Phi = N_m \, \mathrm{F2}_{(c)} / N_m \, \mathrm{F2}_{(a)} \qquad (1)$$

where $N_m \, \mathrm{F2}_{(a)}$ is the electron density at the F2 peak observed by the Alouette satellites and $N_m \, \mathrm{F2}_{(c)}$ is its value predicted by the CCIR model.

The model variation of Φ used was basically that adopted by H and N. To avoid the effects of discontinuities in the gradient of Φ at the top and base of each wall, the linear walls in the model of H and N were replaced with a cosinusoidal increase up to the constant maximum value of Φ_m. In addition to this trough in the $F2$ peak density, a similar one in the peak height was also included, in that it was raised by an amount Δh inside the trough; Δh was given the same model variation as Φ, with values of the maximum Δh_m of up to 50 km and coincident with the maximum depletion [*Lockwood*, 1980]. The layer semithicknesses were assumed constant across the trough. This model of the trough is demonstrated (for the conditions of Figure 1) by the electron density contours shown in Figure 2 (as a function of height, local time, and invariant latitude, and viewed from below the F layer). The contours are for an electron density of 4×10^{10} m^{-3}. At a lower density the trough would appear less deep, and at a higher value the contours are no longer continuous, because the $F2$ peak density in this particular example is reduced to just over 4×10^{10} m^{-3} inside the trough.

This model of the trough gives a qualitative explanation of the observed power losses. The value of the power losses were often found to be very low during magnetically quiet nights. By comparing the observed losses with minimized terms in the total sky wave loss prediction, a minimum estimate of the focusing gain, G_m, (due to a nonspherical reflecting layer, for example) was obtained [*Lockwood and Mitchell*, 1980]. The variation of G_m for
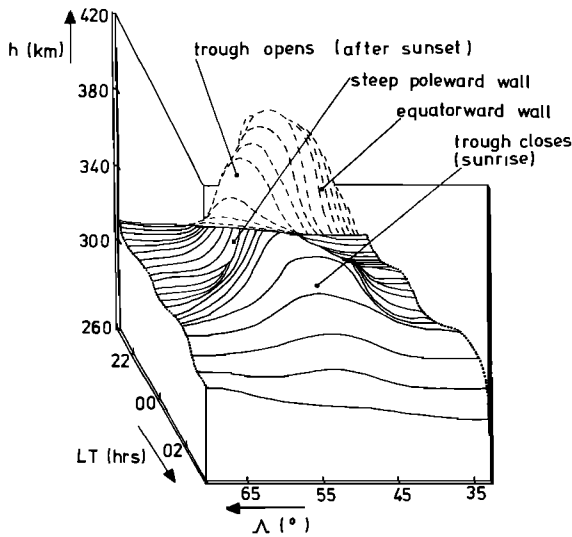
Fig. 2. Contours of electron density of 4×10^{10} m^{-3} for the model trough under the conditions of Figure 1.

near a reflection point. Furthermore, this comparison is quite successful over the range of K_p values for which the trough remains at the latitudes of this path. Other examples are given in Figure 4. The limitations of the model are, however, shown by comparison of Figures 4c and 4d. These two nights, which have similar K_p values, yield almost identical model variations but dissimilar G_m observations.

In a 3-month period in 1976 (April, May, and June), 40% of all readings when the path was entirely in darkness gave G_m values exceeding 10 dB. However, no positive G_m values were obtained at times when the mean K_p exceeded 2.75, and there is a sharp cut-off in G_m about this value (Figure 5). Regular G_m observations are only available for April, May, and June 1976. Hourly recordings of the signal-to-noise ratio S of the demodulated signal were, however, made continuously over a period
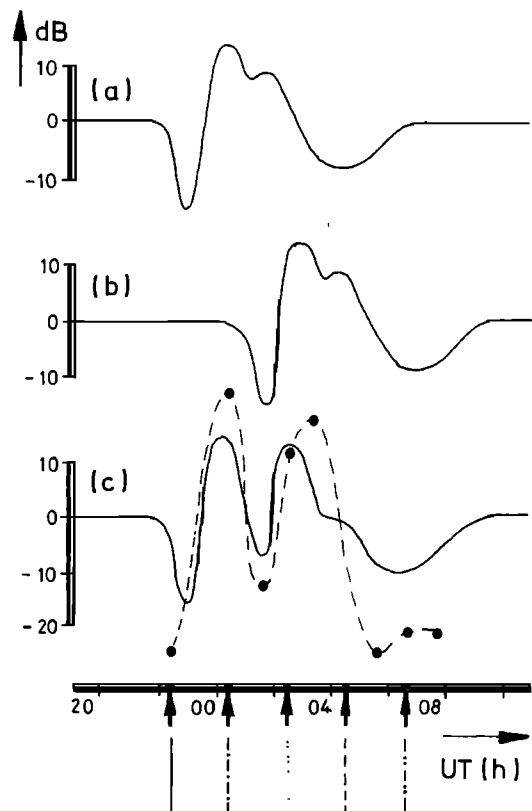
the night of May 18–19, 1976 is shown by the points in Figure 3c. The lowest loss propagation mode predicted at these times was invariably the 2*F*2 mode. Consider an idealised 2*F*2 mode with ionospheric reflections near the points A and B of Figure 1. Figure 3a shows the smoothed focusing gain variation produced by the ray-tracing model for the first of the two equal-length hops. The codings below the UT scale refer to the different relative orientations of the path and trough shown in Figure 1. As the point A nears the edge of the sunset end of the trough, the rays are first defocused and then focused by the convex and concave reflecting layer curvatures, respectively [*Helms and Thompson*, 1973]. This effect then recurs in reverse order as the point A exits from the trough area. The effect of the sunrise end of the trough is the smaller, as it is less steep. Prior to this, the same 'signature' was caused by the motion of point B through the trough region, Figure 3b. The total gain is shown in Figure 3c, and it can be seen that it is very similar to the observed variation despite the simple and two-dimensional nature of the model. The observed values of G_m are generally a little larger than the model predictions, but this difference can be ascribed to lateral focusing gain. This would occur in the plane perpendicular to the propagation path and would be added to the longitudinal gains shown in Figure 3 at times when the trough is open

Fig. 3. Two-dimensional focusing gain predicted for the night of May 18–19, 1976 for the first hop (*a*), the second hop (*b*), and both hops (*c*) of an idealised 2*F*2 mode. Observed values of the gain G_m are shown as points in 3*c*.
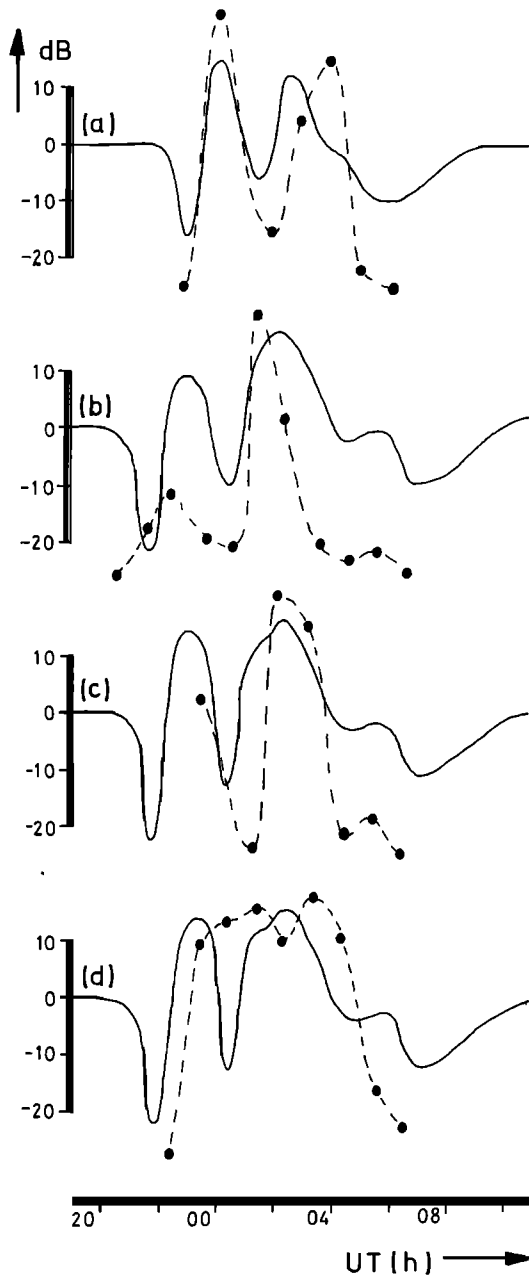
Fig. 4. Modelled and observed focusing gains for (a) May 17–18 ($\bar{K}_p$ = 0.5), (b) April 23–24 ($\bar{K}_p$ = 2.2), (c) April 22–23 ($\bar{K}_p$ = 2.6), (d) April 24–25 ($\bar{K}_p$ = 2.5).

of 17 months, and the diurnal variations of the monthly means of S are shown in Figure 6. The arrows indicate the times between which the mean predicted trough would be fully open at point A or point B, if it is at the latitudes of these points.
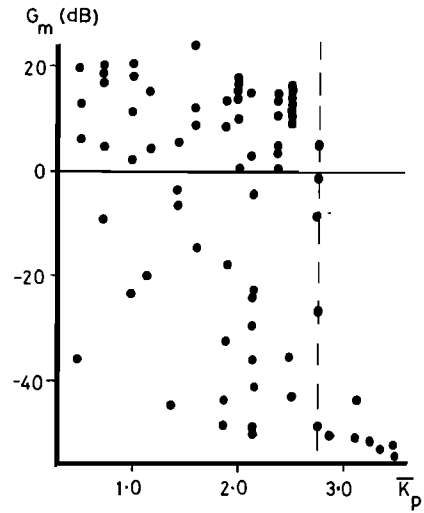

Fig. 5. Focusing gain G_m as a function of the mean K_p value on the night of recording.

It can be seen that in all 17 cases these times correspond quite closely to peaks in the diurnal variation.

Figure 7 shows the regression line for the solar zenith angles at which S drops below +3 dB at sunrise, χ_1, as a function of the K_p value. Also
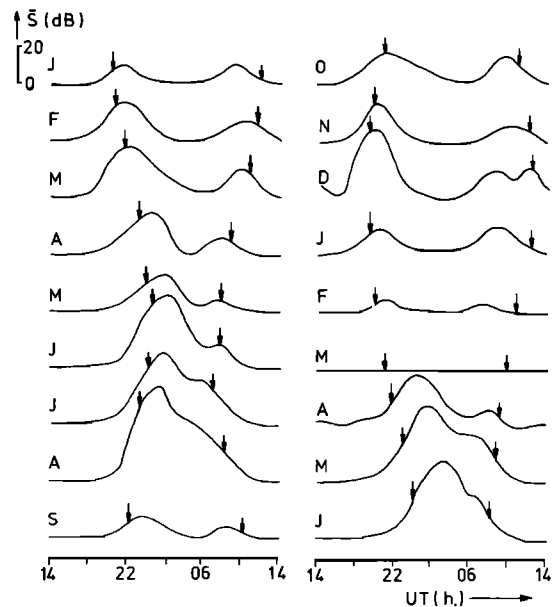

Fig. 6. Diurnal variations of the monthly means of the signal to noise ratio $\bar{S}$ for January 1976 to June 1977. The arrows indicate the times that the mean trough is predicted to open at B and close at A.
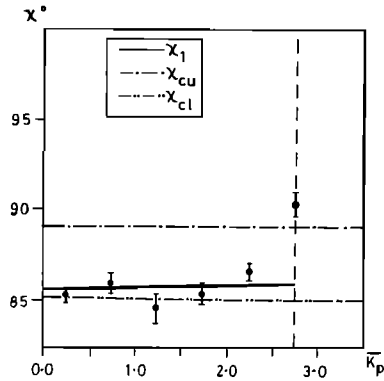
Fig. 7. Regression line of the solar zenith angle χ_1 and the limits of the angle χ_c, χ_{cl}, and χ_{cu} (see text) as a function of K_p. The points are the mean values of χ_1 in K_p ranges of 0.5, plus and minus 1 standard error.

Fig. 9. Observed (points) and predicted Doppler shift variations for the night of June 5-6, 1977 ($\bar{K}_p = 1.4$) for $\Phi_m = 4.0$ and various values of Δh_m (km).

shown are χ_{cu} and χ_{cl}, the limits of the zenith angle χ_c, at which the mean predicted trough ceases to be fully opened at the point A. The slope of the regression line is $0.1° \pm 0.8°$, hence χ_1 is independent of the K_p value, as is χ_c. Within experimental accuracy the two coincide, although the signals tend to fall below 3 dB shortly after (lower χ) the trough begins to close at A.

In Figure 8 the solar zenith angle lagged by 1.5 hr of local time is used to enable direct comparison with the results of H and N. The slope of the regression line of χ_2', the lagged zenith angle at which S first exceeds 3 dB after sunset, is $-2.2° \pm 1.3°$. This agrees well with the slope of $-3.0° \pm 0.5°$ found by H and N for χ_0', the lagged angle
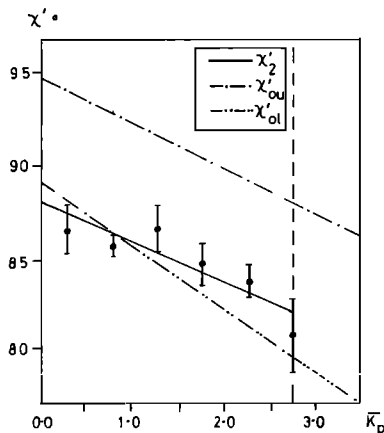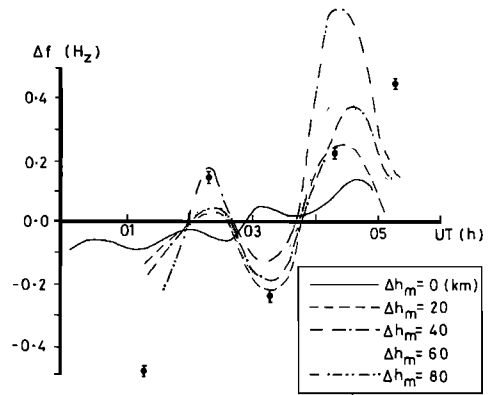

Fig. 8. Regression line of the lagged solar zenith angle χ_2' and trough prediction limits χ_{ou}' and χ_{ol}' (see text).

at which the trough becomes fully opened at point B. (The limits of χ_0' are χ_{0l}' and χ_{0u}'.) At nearly all K_p values, χ_2' and χ_0' coincide to within experimental accuracy, but there is a tendency for χ_2' to be closer to χ_{0l}', so S rises above 3 dB shortly before the trough opens at B. The anticorrelation of χ_2' with the K_p index value is significant at over the 95% level.

Examples of predicted and observed Doppler shift (Δf) variations are shown in Figure 9. The predictions are for various values of the maximum rise in the $F2$ peak height Δh_m and a maximum depletion factor Φ_m of 4.0 as quoted by H and N. It can be seen that it is necessary to include a raised $F2$ peak inside the trough in addition to the depletion to explain the results. A value of Δh_m of the order of 50 km gives Δf predictions that are quite close to the observations.

3. DISCUSSION AND CONCLUSIONS

The times at which the received signal amplitudes rise and fall agree well with the times that the trough is predicted to open and close near the reflection points of the path. The variations of these two sets of times with the K_p index value are also the same. The largest gains would occur near these times, because then focusing would occur in planes both parallel and perpendicular to the path [*Nygrén*, 1977]. The first of these two maxima would be the larger, since the end of the trough is less steep at sunrise than at sunset. The assumption that the base of the trough has a constant depletion of Φ_m

is a simplification. The trough has been reported to be deepest at a variety of local times, but *Brinton et al.* [1978] found the maximum depletion during quiet periods occurred in the post-dusk sector. This would also tend to make the first maximum the larger of the two. All these features can be identified in Figure 6, so the trough offers a good qualitative explanation of the behaviour observed.

Figure 5 shows that the additional gain G_m falls off sharply at a K_p of 2.75. At this activity the locus of A lies close to, or inside, the poleward wall, as is shown in Figure 10. At higher K_p values the point A would remain to the north of the trough all night, because the poleward wall moves equatorward and becomes steeper with increasing activity. This agrees well with the G_m observations, since the first hop would therefore be focused at K_p values below 2.75, but above this value it would be defocused [*Helms and Thompson*, 1973]. At values of K_p just below 2.75 the point A would initially be within the trough, but because the poleward wall moves equatorward with local time, A would pass through it. This may explain the premature cessation of large signal amplitudes near the K_p of 2.75, as is shown by the larger mean value for the $2.5 \leq K_p < 3.0$ range in Figure 7 and the difference between Figures 4c and 4d. At K_p's near 2.75 the first peak is usually still observed, but above this value, either G_m values are low or S is so low that useful recordings cannot be made. Above 2.75 this first peak is not always observed, and if present, the peak G_m values are negative and generally get smaller with increasing K_p. This reduction of the first peak is not predicted by the hypothesis outlined here, since at this time the trough is not yet open over the second hop. This effect may be due to a reduction in the focusing gain due to the narrowing of the trough. It is more
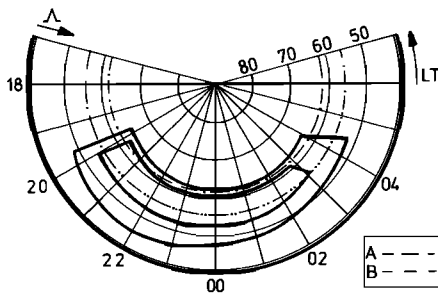
likely, however, that the motion of the sunset end to lower zenith angles causes the peak to shift to times when the nondeviative absorption is higher, and this causes S to become too low for the sensitivity of the apparatus.

The model was only successful in explaining the diurnal Δf and G_m variations if the peak height was raised by about 50 km within the trough. It was noted that both Δf and G_m tended to lag behind their predictions by a delay that varied by up to three-quarters of an hour, but which was usually of the order of 20 min. This raises the possibilities that the positions of the trough vary with altitude below the $F2$ peak or that the Δh variation occurs at slightly later times than the one in Φ. These observations can also be noted in the results of other workers, which have been reviewed by *Lockwood* [1980].

REFERENCES

Ahmed, M., R. C. Sagalyn, P. J. L. Wildman, and W. J. Burke (1979), Topside ionospheric trough morphology: Occurrence frequency and diurnal, seasonal, and altitude variations, *J. Geophys. Res., 84*(2), 489–498.

Bradley, P. A., and J. R. Dudeney (1973), A simple model of the vertical distribution of the electron concentration in the ionosphere, *J. Atmos. Terr. Phys., 35*(12), 2131–2146.

Brinton, H. C., J. M. Grebowsky, and L. H. Brace (1978), The high-latitude winter F region at 300 km: Thermal plasma observations from AE-C, *J. Geophys. Res., 83*(10), 4767–4776.

Buonsanto, M. J., M. Mendillo, and J. A. Klobuchar (1979), Ionosphere at $L = 4$: Average behaviour and the response to geomagnetic storms, *Ann. Geophys., 35*(1), 15–26.

CCIR (1966), Atlas of ionospheric characteristics, *CCIR Rep. 340*, Com. Consul. des Radiocommun., Int. Telecommun. Union, Geneva, Switzerland.

Feinblum, D. A. (1973), Hilion–A model of the high-latitude ionospheric F_2 layer, *Tech. Rep., US Army Contr. DAHC 60-71-C-0005*, Bell Lab., Western Electric, Whippany, N. J.

Grebowsky, J. M., J. H. Hoffman, and N. C. Maynard (1978), Ionospheric and magnetospheric 'plasmapauses,' *Planet. Space Sci., 26*(7), 651–660.

Halcrow, B. W., and J. S. Nisbet (1977), A model of F_2 peak electron densities in the main trough region of the ionosphere, *Radio Sci., 12*(5), 815–820.

Hartmann, G. K. (1975), HF and UHF propagation studies of the mid-latitude ionosphere, *Ann. Geophys., 31*(1), 39–51.

Helms, W. J., and A. D. Thompson (1973), Ray tracing simulation of ionization trough effects upon radio waves, *Radio Sci., 8*(12), 1125–1132.

Köhnlein, W., and W. J. Raitt (1977), Position of the mid-latitude

Fig. 10. Λ-LT plot of mean trough for $\bar{K}_p = 2.75$, May 1976.

trough in the topside ionosphere as deduced from ESR04 observations, *Planet. Space Sci., 25*(6), 600–602.

Lockwood, M. (1980), The bottomside mid-latitude ionospheric trough, *J. Atmos. Terr. Phys., 42*(7), 605–615.

Lockwood, M., and V. B. Mitchell (1980), Oblique HF radiowave propagation in the main trough region of the ionosphere, *Radio Electron. Eng., 50*(11/12), 559–566.

Mendillo, M., and C. C. Chacko (1977), The baselevel ionospheric trough, *J. Geophys. Res., 82*(32), 5129–5137.

Mendillo, M., C. C. Chacko, F. Lynch, and P. J. L. Wildman (1978), Attempts to predict trough/plasmapause boundaries in real time, *Spec. Rep. 212, AFGL-TR-78-0080,* Air Force Geophys. Lab., Cambridge, Mass.

Nygrén, T. (1977), Simulation of vertical incidence ionograms by ray tracing method in the presence of replacement layer and ionospheric trough, *J. Atmos. Terr. Phys., 39*(6), 733–739.

Schunk, R. W., P. M. Banks, and W. J. Raitt (1976), Effects of electric fields and other processes upon the high-latitude *F* layer, *J. Geophys. Res., 81*(19), 3271–3282.

Spiro, R. W., R. A. Heelis, and W. B. Hanson (1978), Ion convection and the formation of the mid-latitude *F* region ionization trough, *J. Geophys. Res., 83*(9), 4255–4264.